Model Development and Implementation of a Membrane Shift Reactor

Johannes Völler*, Michael Follmann, Christoph Bayer and Thomas Melin
RWTH Aachen University, AVT - Chemical Process Engineering, Germany
*Corresponding author: johannes.voeller@avt.rwth-aachen.de

Abstract: Low temperature fuel cells require hydrogen of high purity for electricity production to avoid catalyst poisoning. To purify hydrogen-rich flue gases from hydrocarbon steam reforming membrane shift reactors with a metal membranes may be utilized. A model of a tubular membrane shift reactor with a hydrogen-separating palladium membrane is modeled in the COMSOL Multiphysics' Chemical Engineering Module.

Keywords: membrane reactor, palladium membrane, water gas shift reaction

1. Introduction

Fuel cell based **a**uxiliary **p**ower **u**nits (APUs) for trucks are currently one of the most promising mobile applications for low temperature fuel cells. To avoid H_2-storage, the required H_2 needs to be generated on-board by hydrocarbon steam reforming. A conventional APU system is shown in figure 1 (top). It consists of the reforming unit, which generates H_2 and CO by steam reforming of hydrocarbons. CO is a catalyst poison for low temperature fuel cells. Its content is reduced in two shift stages (high temperature shift, HTS, and low temperature shift, LTS) by the water gas shift reaction (eq. 1). The remaining CO is oxidized in a selective oxidation unit.

The disadvantage of such a system is not only its high complexity (number of components) which leads to complicated process control, but also the H_2-losses in the final CO cleaning step causing a significant efficiency drop. Therefore, a shift reactor with an integrated metal membrane for separation of pure H_2 from the synthesis gas is investigated. The shift reactor is expected to reduce system complexity and to increase efficiency.

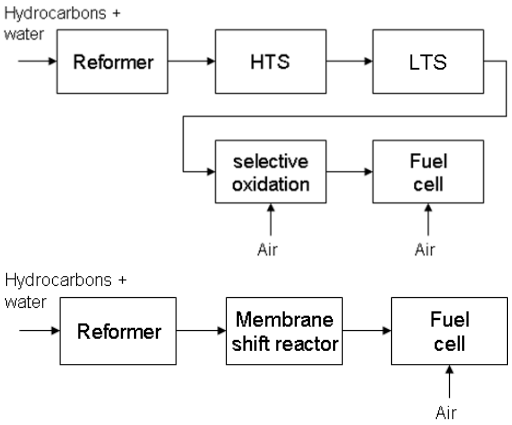

Figure 1. Conventional fuel cell based APU system (top) and membrane shift reactor based system (bottom)

2. Membrane reformer

The membrane shift reactor is built as a double annulus as shown in figure 2. The inner annulus is filled with metal foam coated with catalyst. Synthesis gas generated by steam reforming contains H_2, H_2O, CO, CO_2, and CH_4 in thermodynamic equilibrium. It is fed to the inner annulus of the shift reactor in which CO is converted to H_2 according to the water gas shift reaction (WGS) (eq. 1)

$$CO + H_2O \quad <=> \quad H_2 + CO_2 \qquad [1]$$
$$\Delta H_r = -41 \text{ kJ/mol}$$

Methane is converted to H_2 and CO according to the methane steam reforming reaction (eq. 2).

$$CH_4 + H_2O \quad <=> \quad 3\ H_2 + CO \qquad [2]$$
$$\Delta H_r = 206.2 \text{ kJ/mol}$$

Simultaneously, H_2 is removed across the metallic membrane, which is impermeable for all other species. The reaction equilibria of the WGS reaction and the methane steam reforming reaction are thus shifted towards H_2, yielding higher CO and CH_4 conversion. In order to reduce the required membrane area, the inner

annulus is pressurized to 5 bar to increase the driving force for H_2 permeation across the membrane. The driving force is increased further by use of superheated steam as sweep gas on the permeate side. The temperature in the membrane shift reactor is about 600°C. The target production rate of the membrane shift reactor is 0.06 kg H_2/hr or 2 kW of thermal energy in hydrogen.

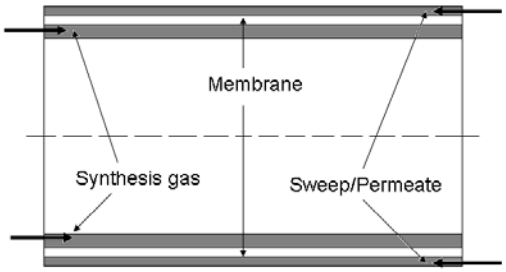

Figure 2. Membrane shift reactor geometry

3. Use of COMSOL Multiphysics

COMSOL Multiphysics with its Chemical Engineering Module was chosen as modeling environment since the differential-algebraic equation system can be easily implemented based on existing models.

3.1 Governing equations

The shift reactor is modeled as two subdomains, the feed side and the sweep/ permeate side, separated by the metal membrane. The model couples equations for mass, momentum and heat transfer to describe the conditions within the reactor.

Feed-side (inner annulus): Pressure loss in synthesis gas flow along the inner annulus is modeled by Darcy's law (eq. 3) to account for the porous metal foam. Diffusive mass transfer takes place especially in radial direction, which is considered with the Stefan-Maxwell-Diffusion equations (eq. 4). To account for temperature changes, heat transfer by convection as well as conduction is considered. Heat generated by chemical reactions within the reactor is included into the equations using adequate heat source terms (eq. 5). H_2-permeation across the metallic membrane is described by Sievert's law (eq. 6 and 7), which was shown to be applicable especially for Pd-based metal membranes (Matthias 2009). The reaction kinetics of the WGS reaction (eq. 8) and the methane steam reforming reaction (eq. 9 and 10) as well as the calculation of the equilibrium constants (eq. 11 and eq. 12) are based on literature data.

Momentum transport

$$\nabla \cdot \left(-\rho \cdot \frac{\kappa}{\eta} \nabla p \right) = F \qquad [3]$$

Mass transport

$$\nabla \left(\begin{array}{l} \rho\omega_i \left(-\rho \cdot \frac{\kappa}{\eta} \nabla p\right) - \rho\omega_i \cdot \\ \cdot \sum_{j=1}^{n} \tilde{D}_{ij} \left(\nabla x_j + \left(x_j - \omega_j\right) \frac{\nabla p}{p} \right) \end{array} \right) = \sum \left(\nu_i R\right) \qquad [4]$$

Heat transport

$$\begin{array}{l} \nabla \cdot \left(-k \nabla T\right) + \left(\rho C_p\right) \left(-\rho \cdot \frac{\kappa}{\eta} \nabla p\right) \cdot \nabla T \\ = -\sum \left(\Delta H_r \cdot R\right) \end{array} \qquad [5]$$

H_2 permeation across membrane

$$F = Q_{H_2}(T) * A \left(\sqrt{p_{H_2}^F} - \sqrt{p_{H_2}^P} \right) \qquad [6]$$

$$Q_{H_2}(T) = Q_0 \cdot \exp\left[\frac{E}{R} \left(\frac{1}{T_0} - \frac{1}{T} \right) \right] \qquad [7]$$

Water gas shift reaction (Sommer 2002)

$$\begin{array}{l} R_{WGS} = k_0 \exp\left(\frac{-E_A}{RT} \right) p_{CO}^a p_{H_2O}^b p_{H_2}^c p_{CO_2}^d \cdot \\ \cdot \left(1 - \frac{y_{H_2} y_{CO_2}}{y_{H_2O} y_{CO} K_{WGS}(T)} \right) \end{array} \qquad [8]$$

Methane steam reforming reaction (Jarosch 2002)

$$R_{CH_4} = \frac{p_{CH_4}}{\left(\theta_1^* + \theta_2^* p_{CH_4}\right)} \left[1 - \frac{p_{CO} p_{H_2}^3}{p_{CH_4} p_{H_2O} K_{CH_4}} \right] \qquad [9]$$

$$\theta_i^* = \theta_{1,i} \cdot \exp\left[\frac{-\theta_{2,i}}{R} \cdot \left(\frac{1}{T} - \frac{1}{T_c}\right)\right] \quad [10]$$

Water gas shift reaction equilibrium constant (Chinchen 1988)

$$\ln(K_{WGS}(T)) = \frac{5693{,}5}{T} + 1{,}077\ln(T) + \\ + 5{,}44 * 10^{-4} T - 1{,}125 * 10^{-7} T^2 - \\ - \frac{49170}{T^2} - 13{,}148 \quad [11]$$

Methane steam reforming equilibrium constant (Farrauto 1999)

$$K_{CH_4}(T) = \exp\left(30{,}345 - \frac{27278}{\mathrm{T}}\right) \quad [12]$$

Sweep / permeate (outer annulus): The sweep / permeate annulus is modeled in a similar manner. Darcy's Law is applied even though the inner annulus is not filled with metal foam, as it greatly facilitates the implementation of momentum change due to hydrogen permeation and its effect on the velocity field. The cost is loss of information about the influence of radial velocity gradients though. No reaction takes place on the sweep / permeate side. Heat and mass transport across the membrane (between the subdomains) is modeled with extrusion coupling variables.

3.2 Boundary conditions and coupling variables

Two rectangular subdomains with three application modes and 5 relevant species require 40 boundary conditions to give a fully specified problem.

Flows in the feed-side and sweep / permeate-side are countercurrent. For the momentum transport, the inlet velocities $u_{1,0}$ and $u_{2,0}$ are given as well as the pressure conditions at the outlet on the opposite side, $p_{1,0}$ and $p_{2,0}$. Influence of hydrogen transport across the membrane on the velocity is accounted for using volumetric source terms. The transport across other boundaries is constrained to zero.

For the heat transport, the inlet boundaries are specified as given temperature levels and the outlets as convective heat fluxes. To couple thermally the two compartments, the trans-membrane heat flux is defined by heat transfer coefficients (eq.13).

$$q_0 = h \cdot (T_2 - T_1) \quad [13]$$

For the mass transport, mass fractions of H_2, H_2O, CO and CO_2 are given at the respective inlets. The mass fraction of CH_4 follows from the condition of unity. The feed stream composition coming from the reformer is assumed to be in equilibrium and calculated by minimizing free Gibbs energy. At the outlet, convective flux conditions are specified for all species. The species cannot permeate through walls, hence, insulation conditions are chosen.

However, hydrogen may permeate through the membrane. Coupling variables are used to calculate the hydrogen flux across the membrane. The hydrogen partial pressures on the feed and the permeate side are calculated at the respective membrane surfaces and mapped onto the surface where the flux is calculated. The flux is mapped back to the other surface to account for both the hydrogen sink and the source in the respective compartments.

3.3 Subdomain settings and coupling variables

The three application modes are strongly coupled. The velocity fields, the temperatures and the pressure levels are determined by solving the momentum, the heat and the mass transfer equations. They in turn influence hydrogen permeation through the membrane, the reaction rates as well as the water gas shift and the methane steam reforming equilibria. Heat generated by the reactions is accounted for as a source term in the heat transfer equations. Further, hydrogen permeation significantly influences the velocity fields in both the feed and the sweep / permeate compartment. The gas density, which is part of all transfer modes, is also temperature and pressure dependent. The solution of this highly coupled multiphysics model requires large damping and thus results in long calculation times.

4. Results

Figures 3 and 4 show qualitatively the two-dimensional concentration distribution of H_2 and CO in the reactor. Figures 5 and 6 give quantitative results for H_2 and CO concentrations cross sections in the middle of the reactor compartments. The H_2 concentration along the membrane decreases due to H_2-permeation, which leads to an equilibrium shift of the WGS reaction and thus a further CO conversion (figure 6).

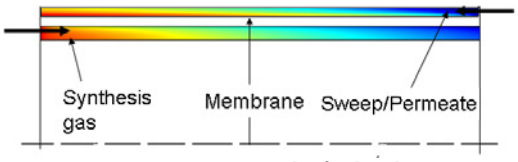

Figure 3. H_2 concentration in the feed and permeate

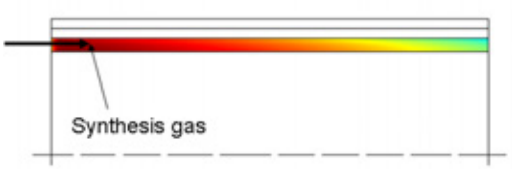

Figure 4. CO concentration in the feed

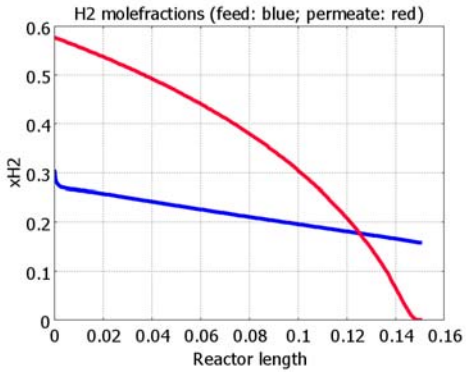

Figure 5. H_2 concentration in the feed stream (blue) and the sweep/permeate stream (red)

Figure 7 shows the hydrogen permeation along the reactor length. Hydrogen permeation across the membrane is highest at the inlet of the feed and the inlet of the sweep respectively. The driving force of hydrogen permeation is the difference in the square roots of the hydrogen partial pressures at both sides of the membrane (figure 8). The widened gap between the curves at both reactor ends illustrates the increased driving force, which explains the peaking hydrogen permeation at the reactor inlets (figure 7).

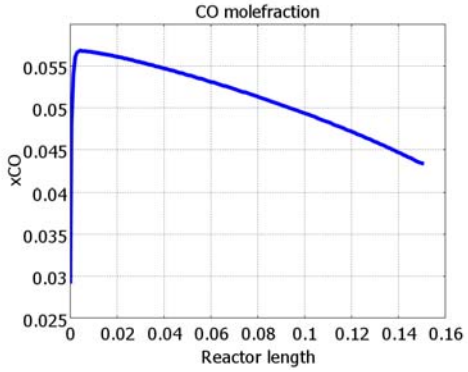

Figure 6. CO concentration in the feed stream

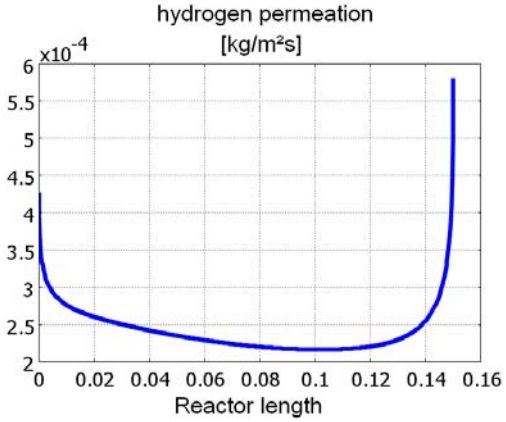

Figure 7. Hydrogen permeation across the membrane

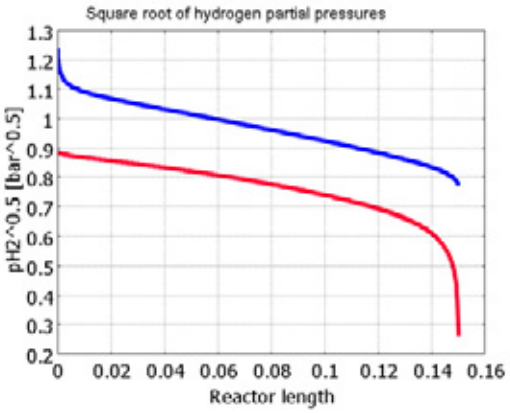

Figure 8. Square root of hydrogen partial pressures at the membrane's feed side (blue) and its permeate side (red)

The results of the COMSOL model are compared to results obtained with a one-dimensional model (1 D) by Matthias (2009). Using feed conditions which result in a (targeted) hydrogen recovery of 0.06 kg/hr with the 1 D-model, the COMSOL model presented predicts only a recovery of 0.033 kg/hr. The difference is due to a much higher methane conversion in the 1 D-model compared to the COMSOL model (70 % to 16 %) The high methane conversion predicted by the 1 D-model prompted the inclusion of the methane steam reforming reaction besides the water gas shift reaction into the COMSOL model of a membrane shift reactor.

The 1-D model is based on the assumption that the feed gas is always in thermodynamic equilibrium. To compare the validity of this assumption within the COMSOL framework, the deviations from equilibrium are computed both for the water gas shift and the methane steam reforming reaction (figures 9 and 10).

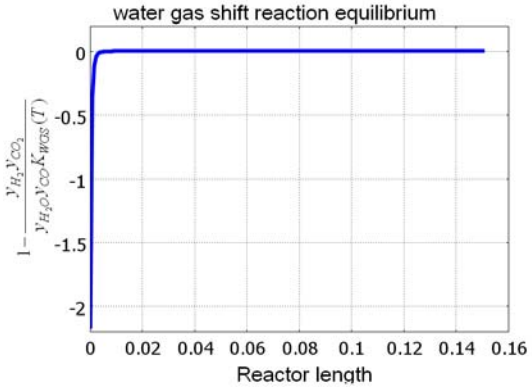

Figure 9. Water gas shift equilibrium

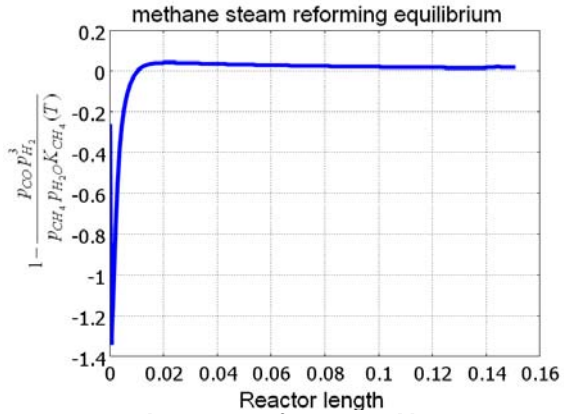

Figure 10. Methane steam reforming equilibrium

The WGS reaction reaches equilibrium virtually instantaneously, but the methane steam reforming reaction deviates significantly. This indicates that the assumption of thermodynamic equilibrium is invalid for the methane steam reforming reaction thus causing much lower CH_4 conversion rates and as a result a lower total hydrogen recovery rate compared to the 1-D model developed by Matthias.

The amount of hydrogen generated by methane steam reforming is 0.0036 kg/hr and thus one order of magnitude smaller than the 0.033 kg/hr of hydrogen that permeates across the membrane. The amount of hydrogen generated in the membrane shift reactor is predicted to be significantly lower using the COMSOL model instead of the 1 D-model. While selective removal of H_2 across the metal membrane influences the equilibria, reaction rates are too low to generate additional hydrogen in significant amounts. Most of the H_2 that permeates through the membrane is generated in the steam reformer upstream of the membrane shift reactor.

5. Summary and Conclusion

The membrane shift reactor implemented in COMSOL Multiphysics indicates that expected methane conversion and hydrogen recovery rates are significantly lower using a non-equilibrium model for chemical reactions. This result has yet to be verified by experiment.

The contribution of the membrane shift reactor to hydrogen yield is low due to low reaction rates. Significant changes in operation parameters and/or geometrical design of the reactor are necessary to achieve a hydrogen recovery rate of 0.06 kg/hr. Parameters that could be improved are a higher reactor volume leading to a higher residence time of the gases in the reactor, changes in temperature to achieve higher reaction rates or a higher membrane area across which more hydrogen is removed from the reactor resulting in higher hydrogen yield.

6. References

1 M. Sommer: *Entwicklung eines Benzinreformers für mobile Anwendungen*, Ph.D thesis, Universität Dortmund (2002)

2. G.C. Chinchen, P.J. Denny: Synthesis of Methanol: Part 1 *Applied Catalysis*, **36**, p. 1-65 (1988)
3. K. Jarosch, T. El Solh, H.I. de Lasa: Modeling the catalytic steam reforming of methane: discrimination between kinetic expressions using sequentially designed experiments, *Chemical Engineering Science*, **57**, p. 3439-3451 (2002)
4. R.J. Farrauto, C.H. Bartholomew: *Fundamentals of industrial Catalytic Processes*, Chapman & Hall London; Weinheim; New York; Tokyo; Melbourne (1999)
5. C. Matthias, *Membrantechnik im Peripherie-bereich von Brennstoffzellenfahrzeugen*, Ph. D. thesis, RWTH Aachen University, (2009)

7. Acknowledgements

The study is part of the AiF project 300 ZN "BtL-Reformer mit Metallmembran". The authors would like to thank the AiF for founding this research.